The Maintenance of High Primary Production in the Absence of Ekman Upwelling: The Supply of Nutrients to the Intergyre North Atlantic

by

Ryan James Peabody

Earth and Ocean Sciences
Duke University

Date:_____

Approved:

_____
M. Susan Lozier, Supervisor

_____
Nicolas Cassar

_____
Zackary Johnson

Thesis submitted in partial
fulfillment of the requirements for the degree
of Master of Science in Earth and Ocean Sciences
in the Graduate School of
Duke University

2018

ABSTRACT

The Maintenance of High Primary Production in the Absence of Ekman Upwelling: The Supply of Nutrients to the Intergyre North Atlantic

by

Ryan James Peabody

Earth and Ocean Sciences
Duke University

Date:_____

Approved:

_____
M. Susan Lozier, Supervisor

_____
Nicolas Cassar

_____
Zackary Johnson

An abstract of a thesis submitted in partial
fulfillment of the requirements for the degree
of Master of Science in Earth and Ocean Sciences
in the Graduate School of
Duke University

2018

Abstract

Ekman suction and pumping are often invoked to explain the observed difference in primary production and chlorophyll *a* between the North Atlantic subpolar and subtropical gyres. Between the gyres, the intergyre region can be loosely defined by its lack of a strong Ekman suction or pumping of nutrients. Despite the lack of a strong Ekman supply of nutrients, the mean seasonal cycle in chlorophyll *a* in the intergyre is remarkably similar to that seen in the subpolar gyre. In this thesis, I present research on mechanisms for nutrient supply to the intergyre that might support its high production. Using biogeochemical and physical reanalysis ocean data products, a nutrient budget is constructed for a region in the eastern North Atlantic, within the intergyre. Analysis of this budget shows that the seasonal entrainment flux, resultant from the seasonal movement of the mixed layer providing access to nutrient-rich waters at depth, is responsible for the majority of the nutrient supply to the region. Hydrographic ocean data and particle trajectories run in a numerical model are then used to show that the waters seasonally entrained into the intergyre mixed layer likely originate in the Gulf Stream, linking nutrient supply in the North Atlantic intergyre to high downstream nutrient fluxes observed in the Gulf Stream.

Contents

List of Tables

List of Figures

Acknowledgments

I would like to express my gratitude to everyone in my life who supported me academically, professionally, and personally during the completion of my degree. Dr. Susan Lozier served as my advisor, and her mentorship and guidance have been invaluable. I am similarly grateful to Dr. Nicolas Cassar and Dr. Zackary Johnson for serving on my committee, and providing valuable feedback as I progressed as a scientist. The other members of our lab have provided similar support, always giving me a group of peers to discuss my work with. Femke de Jong, Kim Drouin, Nicholas Foukal, Feili Li, Laifang Li, and Sijia Zou, you have been fantastic colleagues and friends. Finally, this work would not have been possible without the financial support of the Earth and Ocean Science Division and NASA.

1. Introduction

Marine primary production requires the supply of inorganic nutrients to the illuminated surface waters of the ocean; without nutrients, phytoplankton cannot grow and divide. Phytoplankton growth represents the base of the oceanic food chain, as well as a vital component of the export of carbon from the atmosphere to the deep ocean. To understand the variability in the ocean's biology, it is therefore critical to understand the processes by which the ocean's physics affect nutrient supply, and consequently primary production.

Traditionally, the larger spatial pattern of primary production in the North Atlantic has been attributed to Ekman suction, driven by large-scale atmospheric circulation. Horizontal divergence in the subpolar gyre results in a corresponding vertical supply of water from depth. These waters are enriched in nutrients, fueling strong phytoplankton growth. Conversely, in the horizontally convergent subtropical gyre, Ekman pumping inhibits this supply and phytoplankton growth is low. As a result, annual climatological median surface chlorophyll *a*, a proxy for phytoplankton biomass, roughly correlates with annual climatological mean Ekman upwelling velocities (Figure 1.1). The generally positive velocities in the subpolar gyre are associated with high chlorophyll *a* concentrations, while the generally negative velocities in the subtropical gyre are associated with low chlorophyll *a* concentrations.

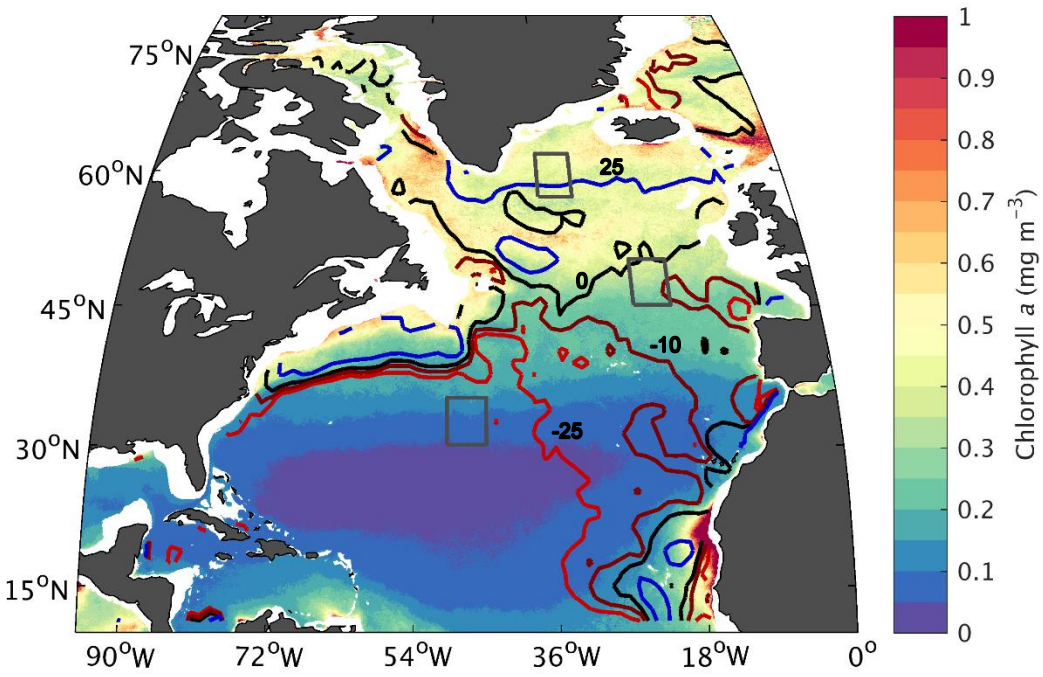

Figure 1.1. Surface chlorophyll *a* concentrations and Ekman upwelling velocities in the North Atlantic. Shading shows climatological annual median chlorophyll *a* concentrations from the ESA Ocean Colour Climate Change Initiative V3.0 dataset (1997-2015). Contours show the -25 m yr^{-1} (red), -10 m yr^{-1} (dark red), 0 m yr^{-1} (black), and 25 m yr^{-1} (blue) Ekman suction velocity isolines, calculated using 1.25° by 1.25° bins of the NOAA Blended Sea Winds dataset. Gray boxes show the boundaries for the regions chosen as the representative subpolar gyre, intergyre, and subtropical gyre in subsequent figures (clockwise from top).

Between the subtropical and subpolar gyres, in the "intergyre region," Ekman velocities weaken and are neither strongly positive nor negative. Despite the lack of a strong Ekman suction-driven supply of nutrients, the climatological seasonal cycle in surface chlorophyll *a* is remarkably similar in both timing and magnitude to the cycle seen in the subpolar gyre [Figure 1.2; *Henson et al.*, 2009]. The research described in this thesis combines observations and model outputs to determine how the nutrients

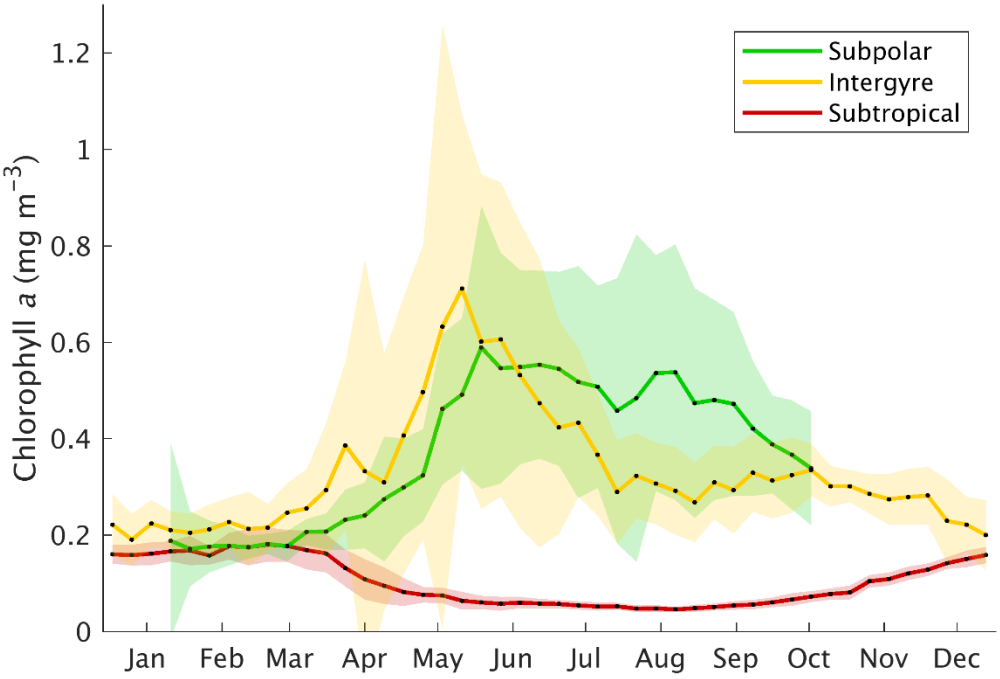

Figure 1.2. Climatological monthly surface chlorophyll *a* concentrations in the subpolar gyre (green), intergyre (yellow), and subtropical gyre (red). Shading shows interannual variability (±1 standard deviation). Data from the ESA Ocean Colour Climate Change Initiative V3.0 dataset (1997-2015). Region boundaries shown in Figure 1.1.

necessary for the observed high primary production in the intergyre are supplied on a seasonal basis.

In the first chapter, the mechanisms controlling nutrient fluxes in and out of a representative region of the eastern intergyre North Atlantic are determined, by calculating the seasonal cycles in nutrient convergences and sinks. This analysis focuses on seasonal supplies of nutrients, to determine the portion of annual new production that can be explained by each flux convergence.

Following results in the first chapter showing the importance of the entrainment flux in supplying nutrients to the mixed layer, the second chapter examines the possible origin of these nutrients in the larger North Atlantic. These results tentatively link the nutrients supplied through the entrainment flux to the Gulf Stream.

2. Nutrient Fluxes in the Intergyre North Atlantic

2.1. Background

While there is debate as to the exact physical controls on primary production in the subpolar gyre, it is generally understood that phytoplankton growth in the subpolar gyre is not limited by nutrients, but rather by light availability and/or zooplankton grazing, which in turn are driven by some combination of mixing and turbulence dynamics [*Behrenfeld*, 2010; *Brody and Lozier*, 2014; *Chiswell et al.*, 2015; *Sverdrup*, 1953; *Taylor and Ferrari*, 2011]. In the subtropical gyre, primary production is limited by nutrient availability; peak growth occurs in winter when strong winds and convective mixing allow access to deeper nutrients, unavailable in the warmer, summer months [*Barton et al.*, 2015; *Gruber et al.*, 2002].

Nutrient fluxes into the mixed layer have traditionally been examined in a vertical framework, in which nutrients are supplied from depth through mixing and upwelling [*Falkowski et al.*, 1998; *Lewis et al.*, 1986]. Though the exact mechanisms responsible for these supplies are still debated, it is commonly held that in nutrient-limited regions of the ocean, increases (decreases) in the vertical supplies translate into increases (decreases) in primary production. Previous work in nutrient-limited regions of the ocean has defied this convention, showing that horizontal fluxes of nutrients do impact nutrient concentrations and primary productions, either through advection [*Dave and Lozier*, 2015; *Dave et al.*, 2015] or mixing [*Letscher et al.*, 2016]. The importance of these

mechanisms is theorized to increase in areas with strong lateral nutrient gradients, including the gyre margins.

Even in a predominantly vertical nutrient supply framework, lateral ocean processes may not be ignored. Nutrients necessary for primary production may be supplied vertically by Ekman upwelling, convective mixing, and turbulent diffusion on seasonal timescales, but over multiple years, export production moves biomass and nutrients into the aphotic zone, and the horizontal introduction of nutrients is necessary to sustain new production. If this horizontal supply was absent, export production would eventually result in a total depletion of nutrients within the mixed layer. This may occur either through the induction of nutrients into the mixed layer along outcropping isopycnals [*Williams et al., 2006*], or through the lateral advection of higher nutrient concentrations into the subsurface nutrient reservoir that is accessed through winter mixing [*Palter et al.*, 2005].

The seasonal cycles in near-surface phosphate, nitrate, and iron concentrations in the intergyre are different than those in the subpolar and subtropical gyres (Figure 2.1, 2.2). Phosphate concentrations in the subpolar gyre decrease from 0.81 μmol L^{-1} in February to a September minimum of 0.49 μmol L^{-1}, while those in the intergyre decrease from a February maximum of 0.41 μmol L^{-1} to a September minimum of 0.11 μmol L^{-1}. Despite the similarity of the magnitude and timing of the vernal phytoplankton blooms in the intergyre and subpolar gyre, nutrient concentrations in the

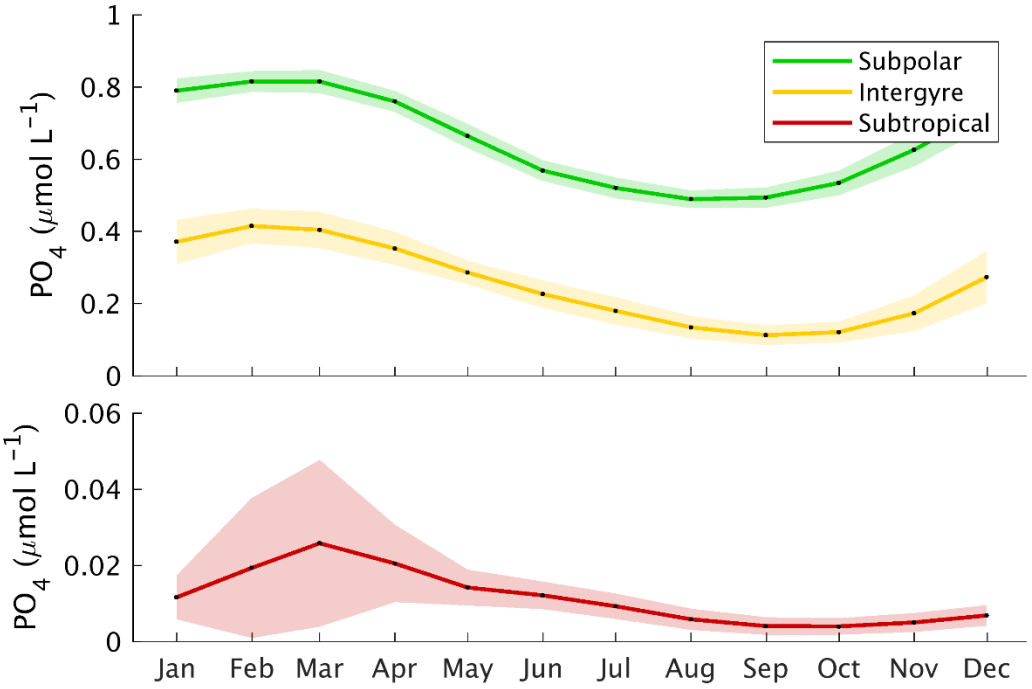

Figure 2.1. Climatological monthly phosphate concentrations averaged over the upper 10 meters of the subpolar gyre (green), intergyre (yellow), and subtropical gyre (red). Top panel shows the subpolar gyre and intergyre, while the bottom panel shows the subtropical gyre (note the different y-axis scale). Shading shows interannual variability (±1 standard deviation). Data from PISCES. Region boundaries shown in Figure 1.1.

intergyre are significantly lower than those in the subpolar gyre. In fact, summer phosphate concentrations in the intergyre are within 0.1 μmol L^{-1} of those seen in the subtropical gyre. Previous work on interannual variability in intergyre phytoplankton blooms (deemed the "transition region") identified years in which phytoplankton bloom initiation was similar to the subpolar gyre, and years in which bloom initiation was similar to the subtropical gyre

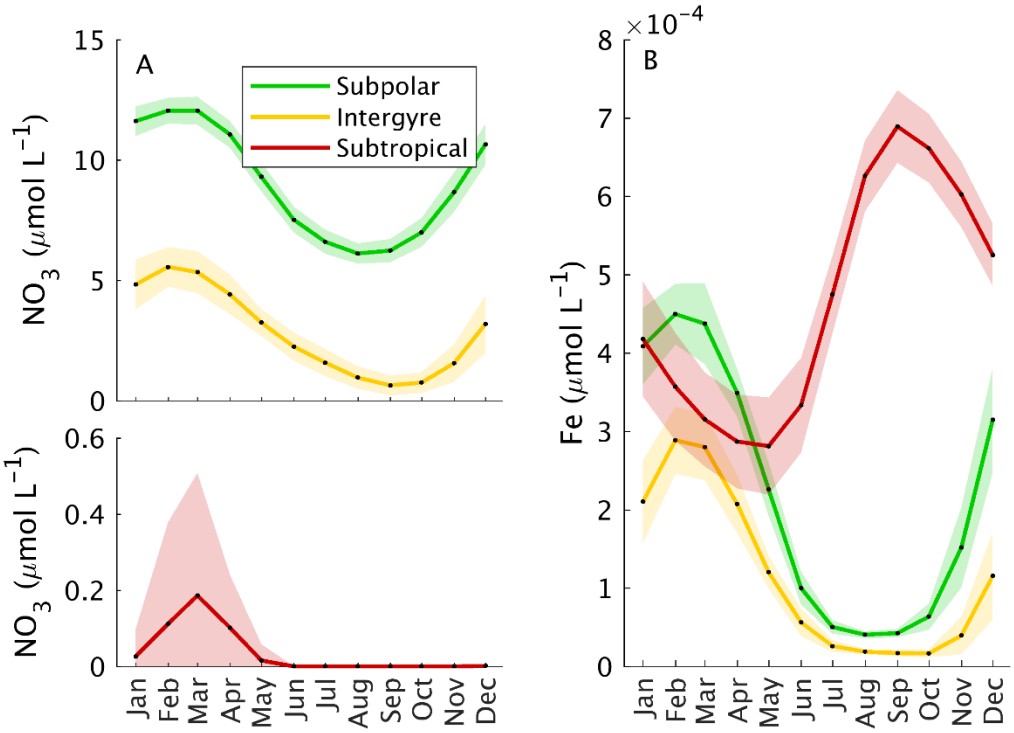

Figure 2.2. A) Climatological monthly nitrate concentrations, and B) climatological monthly iron concentrations averaged over the upper 10 meters of the subpolar gyre (green), intergyre (yellow), and subtropical gyre (red). Shading shows interannual variability (±1 standard deviation). Data from PISCES. Region boundaries shown in Figure 1.1.

[*Henson et al.*, 2009]. In the North Atlantic subtropical gyre, phosphate concentrations of 0.0002-0.001μmol L^{-1} have been deemed low enough to limit primary production [*Wu et al.*, 2000]. The phosphate concentrations seen in the intergyre are over an order of magnitude larger than the values given by Wu et al. [2000], but they are significantly lower than phosphate concentrations in the subpolar gyre. A similar relationship holds true for nitrate concentrations, while extremely low iron concentrations in the intergyre provide some evidence for iron limitation of growth (Figure 2.2). The years in which Henson et al. [2009] observed similar behavior between the intergyre and subtropical

phytoplankton blooms, as well as the relatively low nutrient concentrations observed in the latter, provide tentative evidence that primary production in the intergyre is limited by nutrients to at least some extent. To date, no quantitative estimates of seasonal nutrient fluxes to the intergyre have been made, which may provide valuable insight into the controlling mechanisms on primary production.

2.2. Objectives

Biogeochemical and physical reanalysis data are used to answer the following:

1) What are the dominant sources and sinks of nutrients in the intergyre region?

2) What percentage of annual export production can be each source support?

2.3. Methods

2.3.1. Data and study site

A 5° by 5° region was chosen to represent the intergyre (45°-50° N, 25°-20° W). The intergyre region was chosen so it lay south of the 0 m yr^{-1} Ekman upwelling isoline, as well as within the region described as the "transition region" by Henson et al. [2009]. The regions used to represent the subpolar and subtropical gyres were chosen on the basis of the similarity between the climatological and seasonal patterns in physics (horizontal divergence and Ekman velocity) and biology (primary production and chlorophyll *a*) to those described in the literature.

Nutrient concentrations were obtained from a 0.25° biogeochemical non-assimilative hindcast simulation, based on the PISCES biogeochemical model, giving

monthly outputs from 1998-2014 [*Aumont et al.*, 2015]. PISCES is forced physically by daily outputs from the NEMOv3.1 model, and includes multiple phytoplankton and zooplankton size classes. To estimate horizontal and vertical advective nutrient convergences, surface velocities from the GLORYS2V4 0.25° data assimilative ocean reanalysis were used. The physical forcings of the PISCES hindcast are approximately equivalent to the outputs from GLOYRS2V4, except the latter has data assimilation. Phosphate, one of the two primary macronutrients in the ocean in addition to nitrate, is used for these calculations to reduce possible influences from nitrogen fixation on the stoichiometric relationship between nutrient supply and primary production.

On appropriate timescales, net community production (NCP, defined as gross primary production less autotrophic and heterotrophic respiration) and export production of carbon (and nutrients) to beneath the euphotic depth will be equal. Phytoplankton growth will consume available nutrients, and either result in a decrease in nutrient concentrations, or be balanced by new supplies of nutrients. NCP was estimated using a genetic programming algorithm that maps satellite-derived sea surface temperature and VGPM-derived net primary production (NPP) [*Behrenfeld and Falkowski*, 1997] to observations from an O_2/Ar-based NCP dataset [*Li and Cassar*, 2016]. NPP from PISCES was integrated vertically over the euphotic depth, and treated as satellite-observed NPP, which along with SST from GLORYS2V4 was used to calculate NCP, per Li and Cassar, 2016. Estimates were converted stoichiometrically from units of

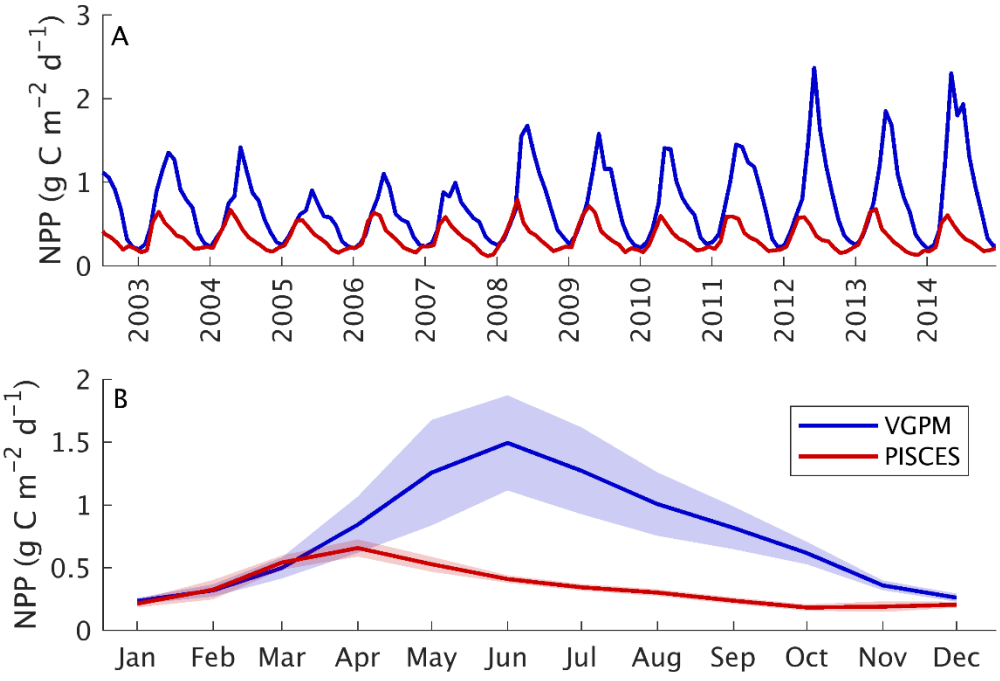

Figure 2.3. A) Depth-integrated net primary production (NPP) in the intergyre, estimated using the VGPM (blue), and PISCES (red). The monthly climatology (B) of both is shown in the lower panel.

carbon and oxygen to phosphate, in order to estimate the phosphate supply necessary to support a given rate of export production [*Redfield*, 1934]. PISCES euphotic depth-integrated NPP is generally lower than that estimated by the VGPM (Figure 2.3). In the absence of an observational validation for NPP (the VGPM estimate itself is a statistical model), the accuracy of one product over the other cannot be readily assessed. Thus, in order maintain consistency with the model physics and biology, NPP estimates from PISCES are used for this study.

Mixed layer depths are calculated as the depth at which potential density is equal to the potential density at the surface, subject to a local 0.8° C temperature decrease [*Kara et al.*, 2000]. The calculation of mixed layer depth has been the source of some debate in the physical oceanographic community, with suggestions ranging from a temperature or density threshold [*de Boyer Montégut et al.*, 2004; *Kara et al.*, 2000], to a comparison of a range of estimates for each profile [*Holte and Talley*, 2009]. Previous work on mixed layer heat balances using a similar mixed layer methodology used a temperature threshold of 1.0° C, and noted that identical results were obtained using a temperature threshold of 0.8° C [*Qu*, 2003].

2.3.2. Phosphate flux calculations

A simple box model was used to represent the intergyre. A conservation equation was used to relate the observed time rate of change of phosphate concentration (referred to as [P] in the equation) within the mixed layer to the convergence of the advective, mixing, and entrainment fluxes of phosphate, less NCP. Monthly flux convergences were calculated over 1998-2014, from which a monthly climatology was computed. In the following equation, overbars denote spatial averaging.

$$\frac{\partial \overline{[P]}}{\partial t} = -\nabla \cdot \overline{\vec{\boldsymbol{u}}_H[P]} - \frac{\partial \left(\overline{w[P]}\right)}{dz} + k_H \overline{\nabla^2[P]} + k_v \frac{\overline{\partial^2[P]}}{dz^2} + \frac{\frac{\int_0^{\overline{MLD}_{t-1}}[P]dz}{\overline{MLD}_{t-1}} - \frac{\int_0^{\overline{MLD}_{t+1}}[P]dz}{\overline{MLD}_{t+1}}}{2\Delta t} + \overline{NCP} \quad (1)$$

To restate the above, the time-rate of change of mixed layer phosphate may be

considered as the sum of the convergence of horizontal advective fluxes, vertical advective fluxes, horizontal diffusive fluxes, vertical diffusive fluxes, the entrainment flux, and sources and sinks (in this case, NCP).

Phosphate time rate of change

$$\frac{\partial \overline{[P]}}{\partial t} = \frac{\overline{[P]}_{t+1} - \overline{[P]}_{t-1}}{2\Delta t} \quad (2)$$

Phosphate concentrations ([P]) are averaged pointwise to the depth of the average mixed layer in the region for each month. For a given month, the time rate of change in phosphate concentration is then the preceding month's phosphate concentration, subtracted from the following month's phosphate concentration, divided by the total elapsed time (two months).

Horizontal advection

$$\nabla \cdot \overline{\vec{\boldsymbol{u}}_H[P]} = \left(\frac{\partial \overline{u[P]}}{\partial x} + \frac{\partial \overline{v[P]}}{\partial y} \right) = \left(\frac{\overline{u[P]_{East}} - \overline{u[P]_{West}}}{\Delta x} + \frac{\overline{v[P]_{North}} - \overline{v[P]_{South}}}{\Delta y} \right) \quad (3)$$

Monthly phosphate concentrations at each region boundary were multiplied pointwise by the normal velocity, and averaged across each boundary, to determine the resultant phosphate fluxes through each face. The differences in phosphate fluxes through opposing faces were then divided by the distance between the faces to estimate the divergence. From here, the convergence (negative divergence) is presented, so positive values result in an increase in phosphate concentrations. A similar convention is used for vertical advection.

Vertical advection

$$\frac{\partial(\overline{w[P]})}{dz} = \frac{\overline{w[P_{MLD}]}}{\overline{MLD}} \tag{4}$$

Assuming nondivergence and 0 velocity at the surface, vertical velocities at the base of the mixed layer can be calculated from horizontal divergence. Pointwise vertical velocities at the base of the mixed layer were multiplied by phosphate concentrations, interpolated pointwise to the base of the mixed layer. Fluxes through the bottom of the region were then averaged and divided by the average mixed layer over the region to calculate the divergence of advective fluxes. As with horizontal advection, convergence (the negative of this term) is discussed from here on.

Horizontal mixing

$$k_H \overline{\nabla^2[P]} = k_H \nabla \cdot \overline{\nabla_H[P]} =$$

$$k_H * \left(\frac{\overline{\left(\Delta[P]/\Delta x\right)_{East}} - \overline{\left(\Delta[P]/\Delta x\right)_{West}}}{\Delta X} + \frac{\overline{\left(\Delta[P]/\Delta y\right)_{North}} - \overline{\left(\Delta[P]/\Delta y\right)_{South}}}{\Delta Y} \right) \tag{5}$$

A horizontal eddy diffusivity coefficient (k_H) of 10^3 m^3 s^{-1} was used [*Abernathy and Marshall*, 2013]. Horizontal phosphate fluxes due to mixing were calculated pointwise across each face of the region, averaged across each boundary, and then used to calculate the convergence of horizontal diffusive phosphate fluxes across the entire region.

Vertical mixing

$$k_v \overline{\frac{\partial^2[P]}{dz^2}} = k_v \frac{\overline{-\frac{\partial[P]}{\partial z}|_{\overline{MLD}}}}{\overline{MLD}} \quad (6)$$

A vertical eddy diffusivity coefficient (k_V) of 10^{-5} m^{-2} s^{-1} was used, previously estimated for the larger North Atlantic thermocline [*Ledwell et al.*, 1997]. Vertical mixing fluxes were calculated pointwise at the base of the region's average mixed layer, averaged spatially, and divided by the average mixed layer to obtain the convergence of vertical diffusive phosphate fluxes.

Entrainment

$$\frac{\frac{\int_0^{\overline{MLD}_{t-1}}[P]dz}{\overline{MLD}_{t-1}} - \frac{\int_0^{\overline{MLD}_{t+1}}[P]dz}{\overline{MLD}_{t+1}}}{2\Delta t} \quad (7)$$

Entrainment is calculated for a given month using the previous and following month's mixed layers, only if the mixed layer deepened over that period. It is assumed that no detrainment flux exists that can change phosphate concentration, so for months in which the mixed layer shoals, the entrainment flux is assumed 0. Average phosphate concentrations are calculated over both mixed layers, using the month of interest's phosphate profiles. The difference in the two concentrations is then divided by the total time between the two months. That is, the entrainment flux is assumed to be equal to the change in phosphate concentration if the mixed layer moved from one depth to another,

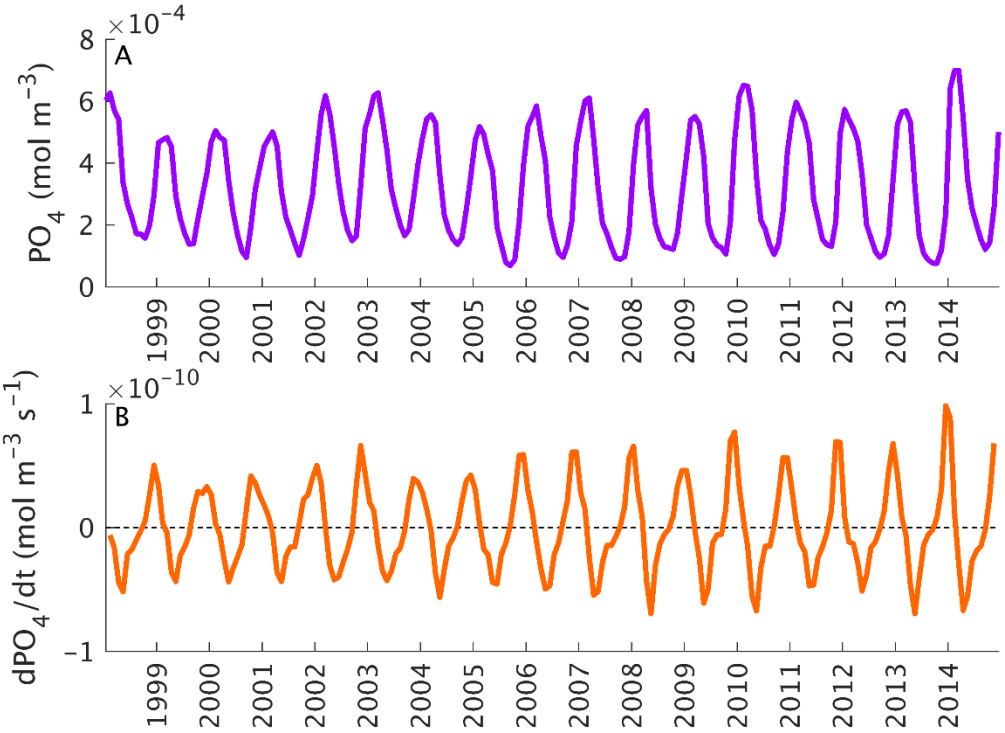

Figure 2.4. A) Average phosphate concentration within the intergyre mixed layer, and B) time rate of change of average phosphate concentration within the intergyre mixed layer.

using a phosphate field that is set for the month of interest, and does not vary with respect to time.

Sources and sinks: NCP

As described in section 2.3.1, mixed layer-integrated NCP is estimated using the Li and Cassar [2016] genetic programming algorithm, converted stoichiometrically from units of mmol O_2 m^{-2} d^{-1} to mol P m^{-2} s^{-1}. To obtain the phosphate sink resulting from NCP within the mixed layer, monthly depth-integrated NCP values are divided by the mixed layer and averaged spatially. Primary production is generally reported as a positive value, but results in the export of nutrients from the euphotic depth, decreasing

phosphate concentrations within the mixed layer. As such, it is always a sink, and values here are given as negative numbers.

2.4. Results

2.4.1. Phosphate flux calculations

Phosphate time rate of change

Average phosphate concentration exhibits strong seasonality, oscillating between approximately 0.5-1.5 mol PO_4 m^{-3} in summer, and 5-6 mol PO_4 m^{-3} in winter (Figure 2.4). The time rate of change of phosphate behaves similarly; each year experiences a period of strong phosphate drawdown, and a period of phosphate replenishment. In the rest of the results section, the full time series of dPO_4/dt will be compared to the sum of the fluxes on the right hand side of equation 1 to determine how well the calculated sources and sinks are representing the time rate of change of phosphate within the mixed layer. With these calculations, we also introduce the residual. The residual is defined as the difference between dPO_4/dt and the sum of the sources and sinks from the original conservation equation.

Advection

The convergence of advective phosphate fluxes is highly variable (Figure 2.5a). Total advective convergence represents a net sink of phosphate over the 16-year time period. This makes sense in the context of our mean picture of the intergyre: there is net downwelling in the intergyre, so there is a net downward vertical mass transport.

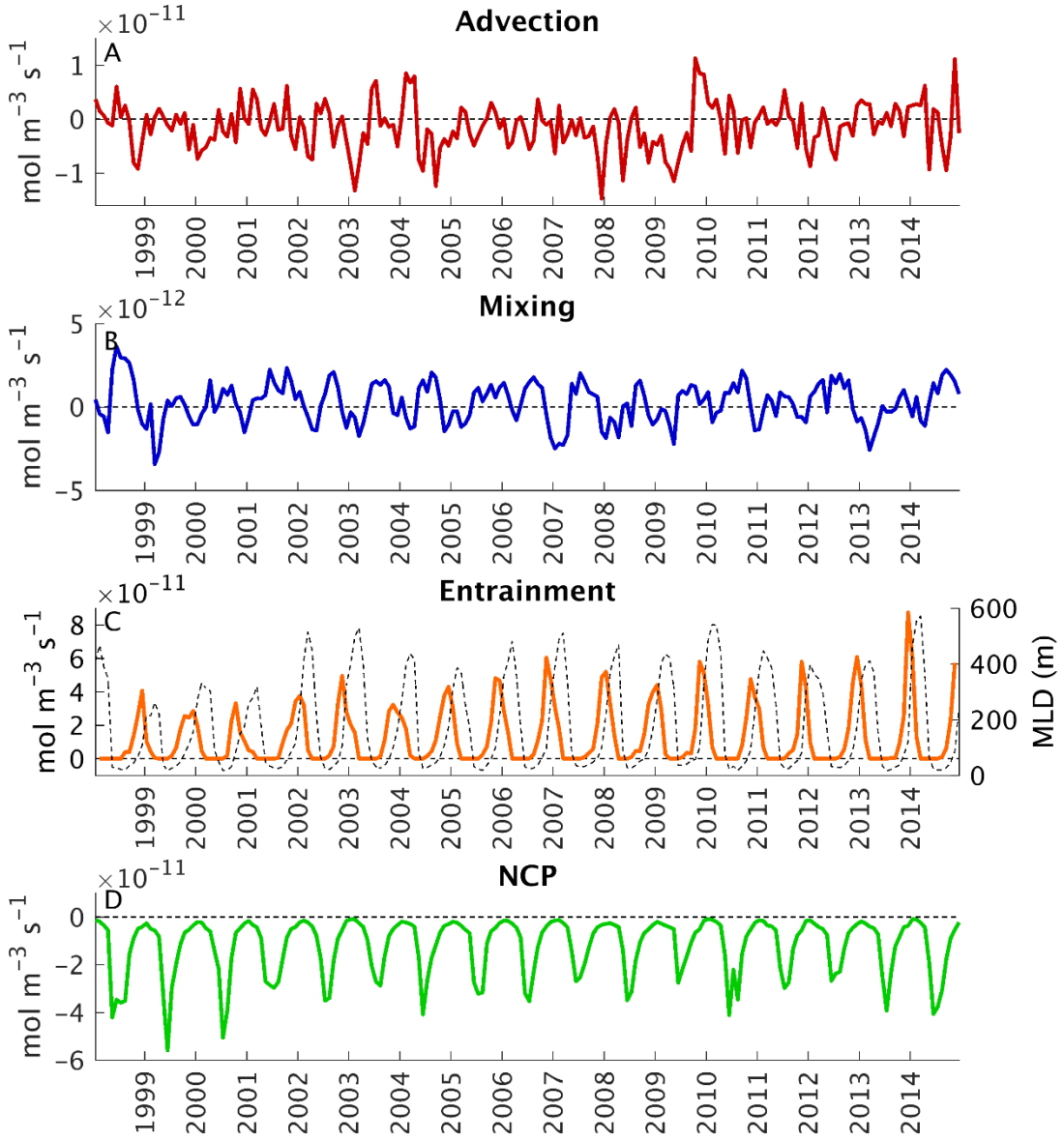

Figure 2.5. Phosphate flux divergences in the intergyre: A) Advective phosphate convergence, B) mixing phosphate convergence, C) entrainment phosphate convergence and mixed layer depth (dashed), and D) net community production (NCP). All fluxes calculated from the PISCES biogeochemical hindcast and the GLORYS2V4 physical reanalysis.

Without strong spatial or temporal variability in horizontal or vertical currents, if the mean vertical gradient in phosphate (increasing with depth) is greater than lateral phosphate gradients, the required conservation of mass will result in a net export of phosphate out of the mixed layer.

Mixing

The convergence of diffusive fluxes is generally smaller than the other phosphate convergences (Figure 2.5b). This is in line with nutrient supply calculated in other regions of the ocean. Dave et al. [2015] found that mixing flux convergences in the Atlantic subtropical gyre were approximately an order of magnitude less than phosphate supply from advection or entrainment, and contributed little to the overall nutrient budget in that region.

Entrainment

The source of phosphate due to entrainment is larger than the sources or sinks due to advection and mixing (Figure 2.5c). Over the 16-year time period, the entrainment flux represents a net supply of nutrients into the mixed layer. This is expected, based on the definition of the entrainment flux in the conservation equation. It is reasonable to assume that nutrient concentrations increase with depth in the open ocean, so deepening the mixed layer in the intergyre will always result in an increase in phosphate concentration.

NCP

NCP is strongly seasonal and always represents a sink of phosphate out of the mixed layer (Figure 2.5d). Average carbon export is approximately 33.4 g C m^{-2} yr^{-1}, which is similar to estimates provided in Li and Cassar [2016] for this region of the ocean, though slightly lower than some of the estimates they present for comparison, namely *Eppley and Peterson* [1979], *Laws et al.* [2000], and *Laws et al.* [2011], all of which estimate intergyre carbon export of approximately 100 g C m^{-2} yr^{-1}.

Full budget

Combining the component nutrient sources and sinks, as per the right hand side of the conservation equation, gives an estimate of phosphate time rate of change within the mixed layer (Figure 2.6). This estimate matches the general seasonal cycle in phosphate time rate of change in terms of summer export and winter accumulation, but it appears that the sources and sinks tend to underestimate the magnitude of maxima and minima, as well as the timing of peak phosphate export. The mean of dPO_4/dt, sources and sinks, and the residual between the two (±1 standard deviation) are as follows: $-4.24 \times 10^{-13} \pm 3.46 \times 10^{-11}$ mol PO_4 m^{-3}, $-5.67 \times 10^{-13} \pm 2.55 \times 10^{-11}$ mol PO_4 m^{-3}, and $1.43 \times 10^{-13} \pm 1.87 \times 10^{-11}$ mol PO_4 m^{-3}, respectively.

2.4.2. Climatological nutrient supplies

The monthly mean of the convergence of advective phosphate fluxes exhibits little seasonality (Figure 2.7a). Due to the processes previously discussed, advective

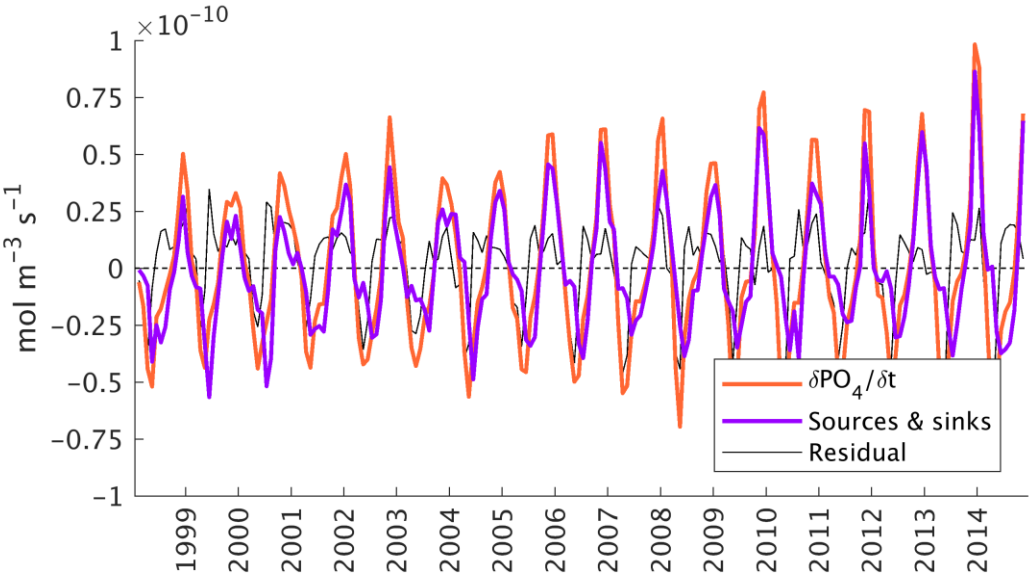

Figure 2.6. Phosphate time rate of change in the intergyre, calculated from average phosphate concentration in the mixed layer (orange), and as the sum of the sources and sinks (purple). The residual is shown in black.

convergence causes a climatological export of phosphate from the mixed layer. Interestingly, there is little seasonality in the magnitude of this export; convergence is weakly negative throughout the year (there is phosphate divergence due to advection). It is worth noting that interannual variability is significantly larger than month-to-month variability, indicating that advection might contribute to interannual variability in the phosphate budget. In contrast, climatological mixing phosphate convergence exhibits strong seasonality (Figure 2.7b). In winter, horizontal gradients in phosphate lead to a divergence out of the mixed layer, while in summer, vertical gradients in phosphate cause a convergence. Interestingly, while monthly advective convergence is larger than advective mixing convergence (Figure 2.5), climatological monthly mean diffusive flux convergence is approximately the same magnitude as climatological

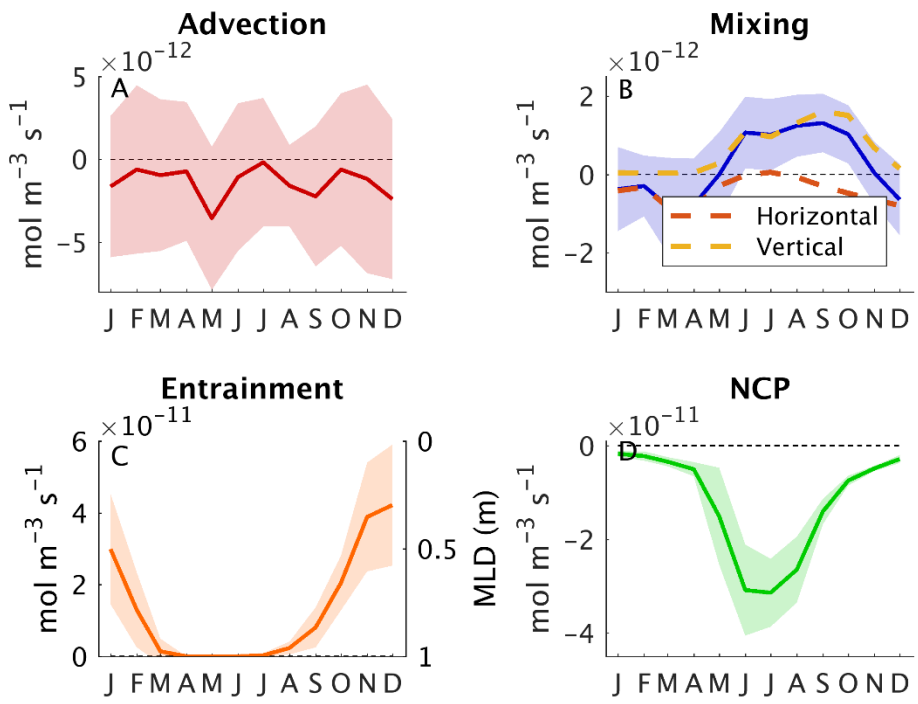

Figure 2.7. Climatological monthly convergence of phosphate in the intergyre due to: A) advection, b) diffusion, c) entrainment, and d) NCP. Shading represents interannual variability (±1 standard deviation). In B) the dashed lines show mixing convergence in the horizontal (red) and the vertical (yellow).

advective convergence, due to the lack of and presence of a seasonal cycle in advective and diffusive convergence, respectively (Figure 2.7). However, neither advective nor diffusive phosphate convergence make as large a contribution to phosphate time rate of change as entrainment (Figure 2.7c) or NCP (Figure 2.7d). Entrainment supplies phosphate to the mixed layer through fall and winter, as the mixed layer deepens. NCP exports phosphate from the mixed layer year-round, with peak export occurring in June and July. There is significant interannual variability in the magnitude of peak export, and peak entrainment.

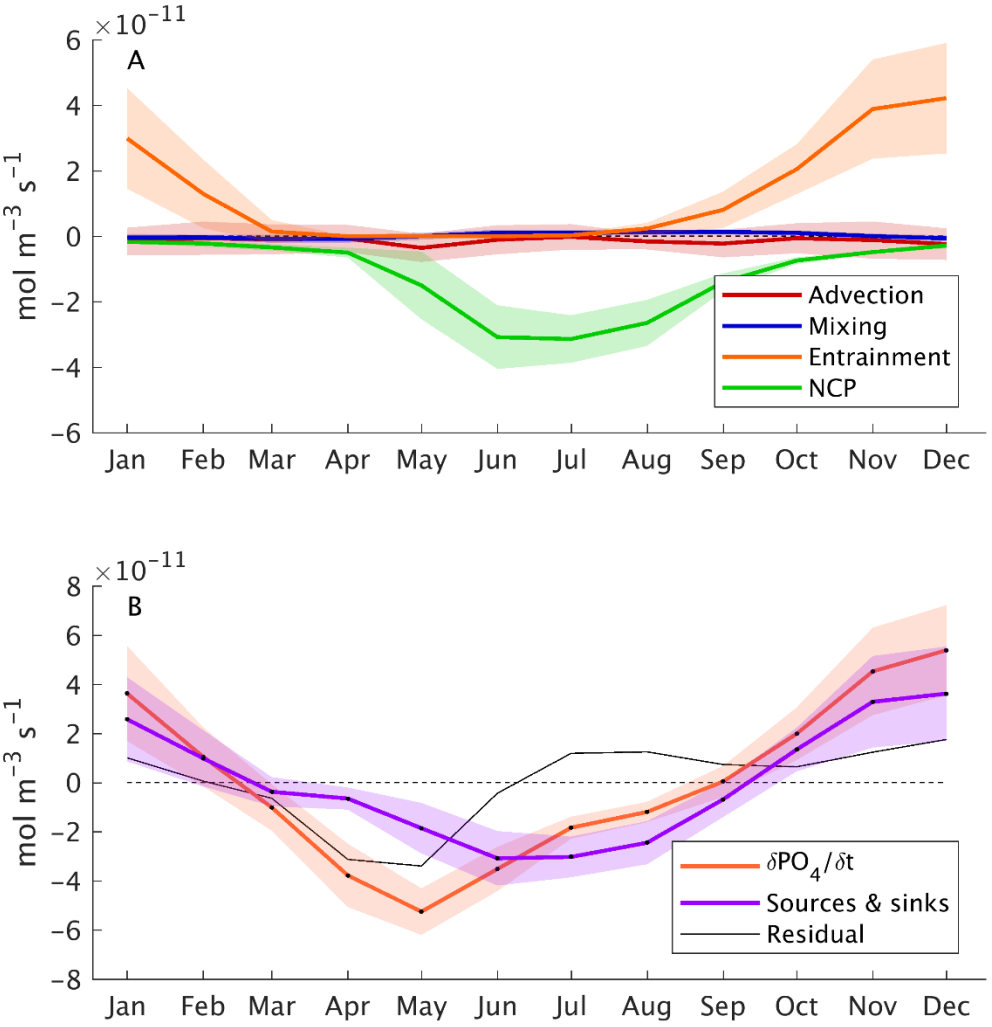

Figure 2.8. A) Climatological monthly phosphate time rate of change, and sources and sinks in the intergyre mixed layer, including the residual (defined as dPO_4/dt, less sources and sinks). B) Phosphate time rate of change, calculated from average phosphate concentration in the mixed layer (orange), and as the sum of the sources and sinks (purple). The residual is shown in black.

Examining all of these fluxes side-by-side make it apparent that the seasonal cycle in phosphate supply is largely controlled by entrainment and NCP (Figure 2.8a). Entrainment and NCP are strongly seasonal, and significantly larger than advective or

mixing convergences. Combining the climatological component nutrient convergences as in section 2.4.1 (Figure 2.6) makes it apparent that the conservation equation is consistently underestimating the magnitude of winter phosphate supply, as well as the magnitude and timing of summer phosphate supply (Figure 2.8b). Average climatological phosphate time rate of change, sources and sinks, and the residual are 2.11×10^{-14} mol PO_4 m^{-3} s^{-1}, -2.14×10^{-13} mol PO_4 m^{-3} s^{-1}, and 2.35×10^{-13} mol PO_4 m^{-3} s^{-1}, respectively.

2.4.3. Contributions to net community production

On average, net community production in the intergyre mixed layer is responsible for the export of 3.82×10^{-4} mol C m^{-3} yr^{-1} (Table 1). The convergence of phosphate diffusion is responsible for a small portion of NCP, fueling 1.9% of the nutrients necessary for new production annually. Overall, entrainment is responsible for the convergence of 4.11×10^{-4} mol PO_4 m^{-3} yr^{-1} in the intergyre mixed layer, supplying more phosphate to fuel than is exported via NCP on an annual mean basis.

Source/sink	NCP	Advection	Mixing	Entrainment
PO_4 supply (mol m^3 yr^{-1})	-3.82×10^{-4}	-4.40×10^{-5}	7.37×10^{-6}	4.11×10^{-4}
Percent of NCP	100%	-11.5%	1.9%	107.8%

Table 1. Climatological mean nutrient sources and sinks, and their contributions to net community production. Each flux convergence is integrated over the year, and also presented as a percentage of total NCP (if the convergence represents a supply). Positive entrainment only considers those months in which entrainment results in an increase in phosphate within the mixed layer.

2.5. Discussion

It is clear that, on seasonal timescales, the entrainment flux and NCP exert a far greater control on mixed layer phosphate concentrations than advective convergence or mixing. The model generally recreates the seasonal cycle of phosphate supply and export, as well as the annual balance between nutrient supplies and export production. On an annual mean basis, calculated supplies and sinks of phosphate are within 2% of NCP. However, the model falls short in several ways, notably the magnitude of peak winter supply, and the timing and magnitude of peak summer export. It is possible that the failure to perfectly capture the amount of winter supply is due to inaccuracy in calculating the mixed layer. The choice of a different density threshold, or metric for the depth of the mixed layer, might result in a change in the entrainment flux. The chosen method for calculating mixed layer gives significantly larger winter mixed layer depths than other methods for calculating mixed layer [*de Boyer Montégut*, 2004; Figure 2.9]. However, using the de Boyer Montégut [2004] mixed layer method increased total carbon export, resulted in a far smaller entrainment flux, and still failed to recreate the timing of peak phosphate decrease (Figure 2.10).

The mixed layer is assumed to be the near-surface layer over which hydrographic properties are homogeneously distributed. Choosing a mixed layer on the

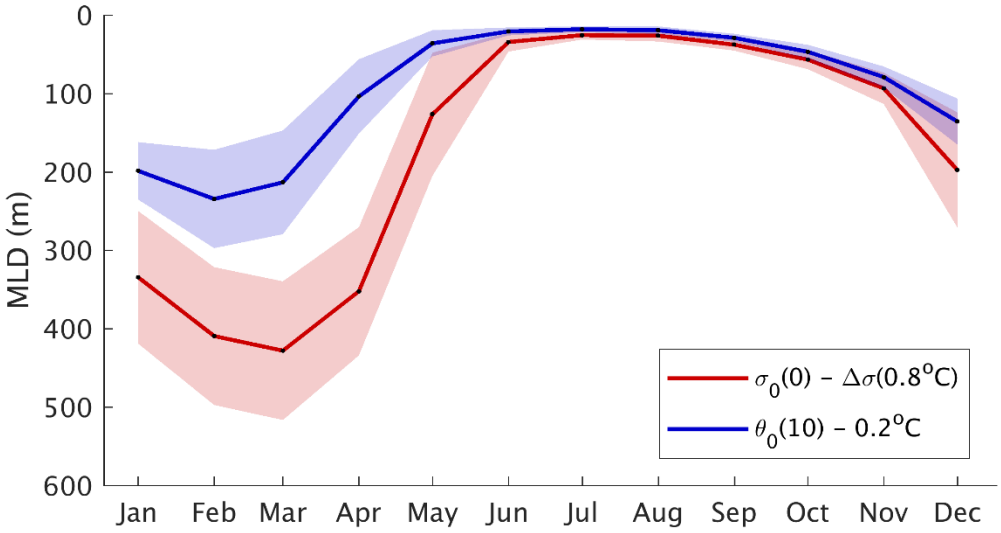

Figure 2.9. Climatological mixed layer depth in the intergyre. Mixed layer calculated using a 0.8° C surface density-temperature threshold (red), and a 0.2° C 10 m temperature threshold (blue), all with GLORYS2V4 data. Shading shows interannual variability (±1 standard deviation).

basis of temperature or density changes will give us a phosphate profile within the mixed layer that is close to homogeneous, but still exhibits some vertical variability. We can see the chosen mixed layer does not give us constant phosphate profiles within the mixed layer (Figure 2.11). Use of a shallower mixed layer gives more uniform phosphate concentrations within the mixed layer. However, the general vertical distribution of phosphate compared to the mixed layer indicates that in PISCES, nutrients are drawn down by production near the surface more quickly than they are distributed throughout the mixed layer. Use of a different mixed layer estimate will not just result in different advection and entrainment terms, but mixing will change (especially in the vertical), as well as the volume divergence of phosphate due to NCP. Using the chosen mixed layer

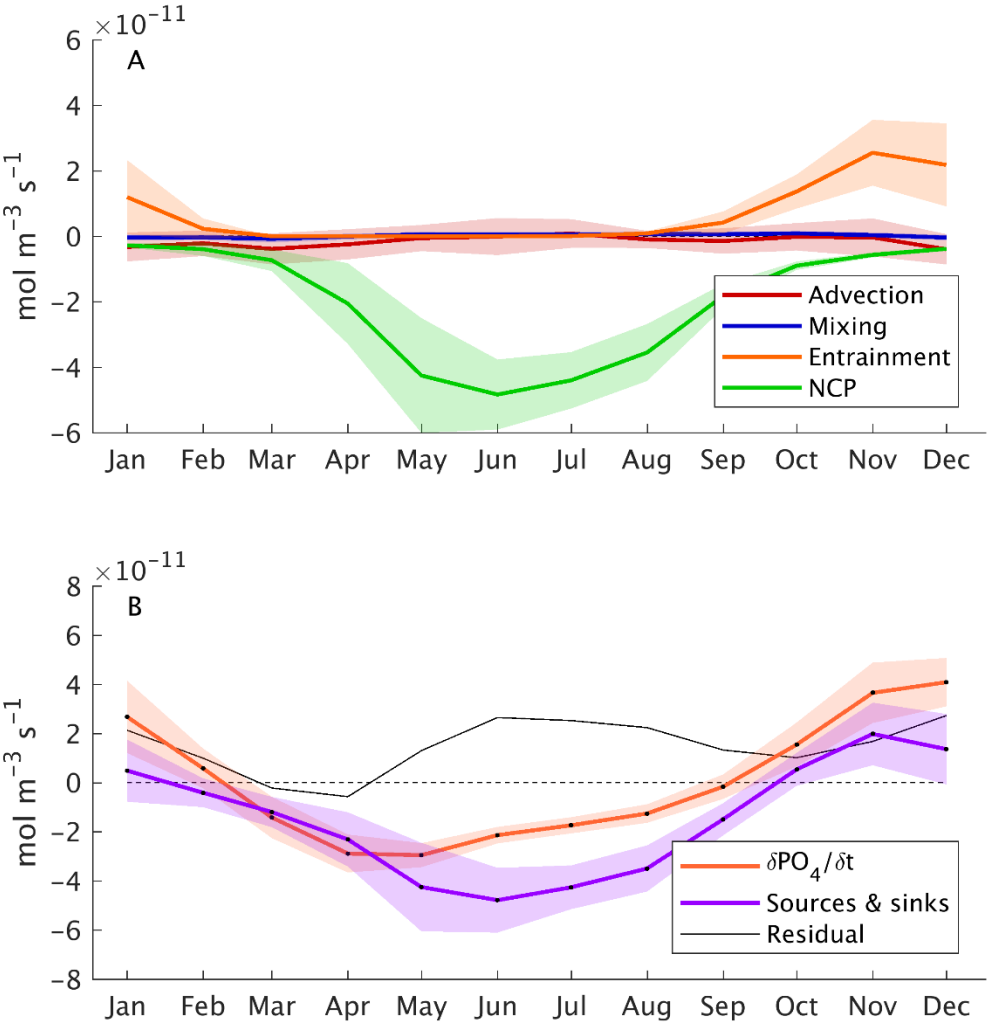

Figure 2.10. A) Climatological monthly phosphate time rate of change, and sources and sinks in the intergyre mixed layer, calculated using a mixed layer depth defined with a $\sigma_0(10)$ - 0.2°C temperature threshold, including the residual (defined as dPO_4/dt, less sources and sinks). B) Phosphate time rate of change, calculated from average phosphate concentration in the mixed layer (orange), and as the sum of the sources and sinks (purple). The residual is shown in black.

method, residual due to winter phosphate supply is significantly smaller than the residual due to the mismatch in export. The root mean squared error of the winter (DJF)

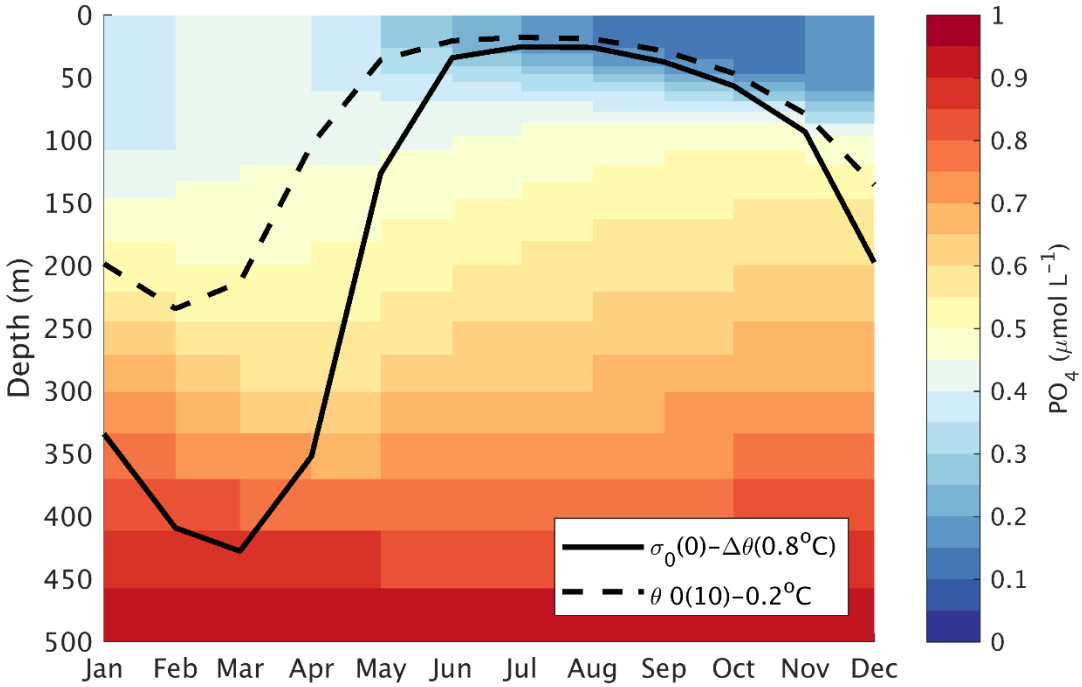

Figure 2.11. Climatological monthly phosphate concentrations and mixed layer in the intergyre. Solid black lines shows the mixed layer calculated using a surface density threshold, while the dashed black line shows the mixed layer calculated using a temperature threshold. All data from PISCES.

residual is 1.17×10^{-11} mol PO_4 m^{-3} s^{-1}, while the root mean squared error of the March-May residual is 2.69×10^{-11} mol PO_4 m^{-3} s^{-1}.

Net community production, by definition, is some percentage of net primary production, dependent on the amount of heterotrophic respiration. The application of the Li and Cassar [2016] algorithm, based on observations, to a model-based dataset, likely introduced some errors in the estimations of phosphate export. Optical models for NCP give a range of estimates for export production in the intergyre, from as low as

approximately 20 g C m^{-2} yr^{-1}, to over 100 g C m^{-2} yr^{-1}. See Li and Cassar [2016] for a full discussion of NCP estimates.

The definition of the mixed layer is also a source of uncertainty. Using a surface density-temperature threshold, the sources and sinks in mixed layer phosphate concentration are at most 8 times smaller in spring, and 2 times larger in fall as the observed time-rate of change when using the surface density-temperature threshold mixed layer (Figure 2.8). Using the temperature threshold mixed layer gives sources and sinks twice the magnitude in summer, and half the magnitude in winter as observed time-rate of change (Figure 2.10).

The use of constant eddy diffusivity coefficients throughout the year introduces another source of uncertainty. In the upper 2000m of the North Atlantic, horizontal eddy diffusivities have been estimated to vary in time by over an order of magnitude [*Cole et al.*, 2015]. Estimates of vertical eddy diffusivities throughout the global ocean are also subject to a large degree of uncertainty and variability: estimates vary by 4 orders of magnitude [*Gregg*, 1987]. As we can only constrain our NCP estimates by approximately a factor of 5, and our mixing convergence by several orders of magnitude, accurate accounting of the true uncertainties in phosphate sources and sinks (NCP, mixing, mixed layer depth) would be larger than the seasonal cycle in the observed time-rate of change in phosphate. Further work is needed to fully explore how each of these assumptions affect the calculation of phosphate sources and sinks.

While further work is certainly needed to quantify the uncertainties in the conservation equation, this work does show that the entrainment flux is responsible for supplying the vast majority of the nutrients necessary for new production. Mixing is only responsible for 3% annually, advection represents an annual loss of phosphate, while entrainment supplies over 100% of the phosphate exported via NCP. Such a result would indicate that interannual variability in winter mixing could drive changes in mixed layer nutrient concentration. This relationship implies a tentative link between variability in winter mixing and variability in primary production in the intergyre on longer than seasonal timescales.

The scope of this study is to determine the mean seasonal cycle in nutrient supplies to the intergyre mixed layer. It is clear that the vast majority of nutrients are supplied by the seasonal movement of the mixed layer, rather than through advection or mixing. For these nutrients to be supplied to the mixed layer, the reservoir beneath the mixed layer must be seasonally replenished, through either export production, or the lateral movement of nutrients into the reservoir itself or the base of the mixed layer [*Palter et al.*, 2011; *Williams et al.*, 2006]. This nutrient reservoir lies between approximately 100 and 400 m, the depths of the summer and winter mixed layers (Figure 2.9). The next section of this thesis will focus on how nutrients might be supplied to these depths via large-scale circulation in the North Atlantic.

3. The AMOC as a nutrient conduit

3.1. Background

3.1.1. The nutrient tube

The general schematic of the Atlantic meridional overturning circulation (AMOC) has long shown the waters of the Gulf Stream connecting through to the subpolar gyre [*Broecker*, 1991]. Such a connection was originally theorized to occur at the surface, based on the observed velocities of surface drifters [*Fratantoni*, 2001]. However, more recent work has shown that such a surface connection does not exist [*Brambilla and Talley*, 2006]. Analysis of surface drifter trajectories revealed that over a sixteen year time period, essentially no drifters were transported from the subtropical to subpolar gyre. Rather, the connection between the subtropical and subpolar gyres occurs at depth [*Foukal and Lozier*, 2017; *Burkholder and Lozier*, 2011; *Burkholder and Lozier*, 2011]. Previous studies, seeding Lagrangian floats in an eddy-resolving model and allowing them to run backward, showed that near-surface waters to the north of the intergyre region originate in the deeper Gulf Stream [*Burkholder and Lozier*, 2014].

Twenty-five years ago, the Gulf Stream was identified as an advective pathway for nutrient transport [*Pelegrí and Csanady*, 1991]. Over five transects across the Gulf Stream, from the Straits of Florida to the offshore Gulf Stream at 40° W, Pelegrí and Csanady [1991] identified a subsurface maximum in downstream nutrient fluxes. Nutrients in the euphotic depth of the Gulf Stream are quickly consumed by

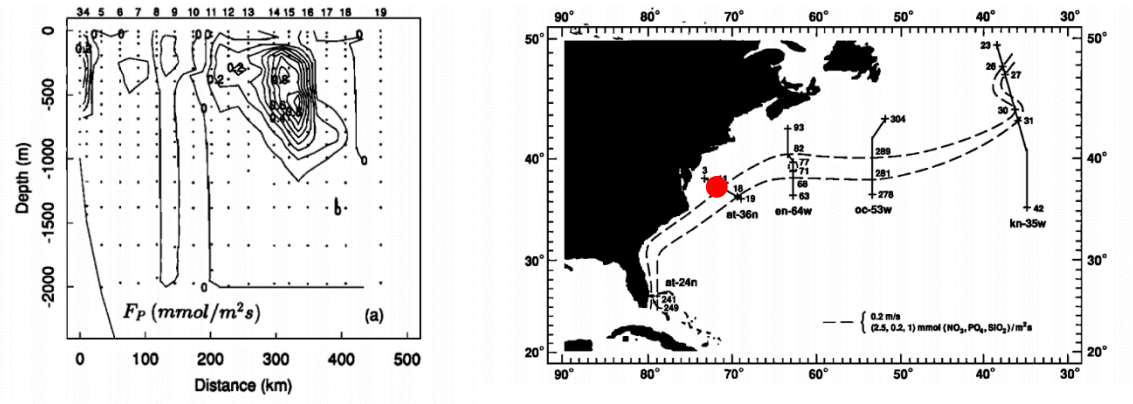

Figure 3.1. The nutrient tube. A) Downstream phosphate fluxes in a cross-stream section of the Gulf Stream, and B) its location (marked with a red dot) in the larger context of the Gulf Stream and the North Atlantic subtropical gyre. Figure adapted from *Pelgrí and Csanady* [1991].

phytoplankton, and concentrations increase only beneath the euphotic depth. Conversely, velocities in the Gulf Stream are elevated at the surface and decrease with depth, giving the downstream nutrient flux an appearance that led Pelegrí and Csanady [1991] to describe it as the "nutrient tube (Figure 3.1). The strongest downstream fluxes are centered on the 26.8 σ_0 isopycnals, at about 500 m depth in the Gulf Stream, extending down to the 27.5 σ_0 isopycnal. Nutrients in the tube likely originate in the tropics or southern hemisphere, implicating the AMOC as a conduit for nutrient transport into the North Atlantic subtropical gyre [*Palter and Lozier*, 2008]. Interestingly, the isopycnals associated with the core of the nutrient tube (26.8-27.5 σ_0) lie at the depths in the Gulf Stream that Burkholder and Lozier [2014] identified as connecting to the eastern subpolar gyre. As these density surfaces move northward, they shoal [*Burkholder and Lozier*, 2011], possibly making the nutrients advected along them accessible through winter mixing at higher latitudes.

Model studies have previously shown that Gulf Stream nutrients are advected from the subtropical gyre to the subpolar gyre and into the base of the winter mixed layer [*Williams et al.*, 2011]. Williams et al. [2011] hypothesized that the nutrient stream splits at the gyre boundary: nutrients on isopycnals lighter than 26.8 σ_0 are recirculated and confined to the subtropical gyre, while nutrients on heavier isopycnals are advected into the subpolar gyre via the AMOC. Despite the evidence for a nutrient throughput from the subtropical to subpolar gyre, to date there have been no efforts to examine the possibility of a nutrient throughput from the subtropical gyre to the base of the winter mixed layer specifically in the intergyre.

3.1.2. Density surfaces outcropping in the intergyre

As nutrient tube isopycnals shoal with increasing latitude, they are mixed to the surface (Figure 3.2). In section 2, we saw that climatological winter mixed layers within the intergyre reach 400 m depth. (Figure 2.9). Examining the winter position of the 26.8-27.1 σ_0 isopycnals shows that density surfaces made available through winter mixing lie as deep as 500-700 m depth in the Gulf Stream, and as deep as 800 m in the core of the subtropical gyre (Figure 3.2). In the average year with mixing down to 400 m, the 26.8-27.0 σ_0 isopycnals are all intersected by the intergyre mixed layer. The 27.1 σ_0 and above isopycnals do not generally intersect the mixed layer, but may be in years with deeper mixing. Some evidence of nutrient conservation along density surfaces is also apparent. Despite the shoaling of Gulf Stream isopycnals toward the surface, elevated nutrient

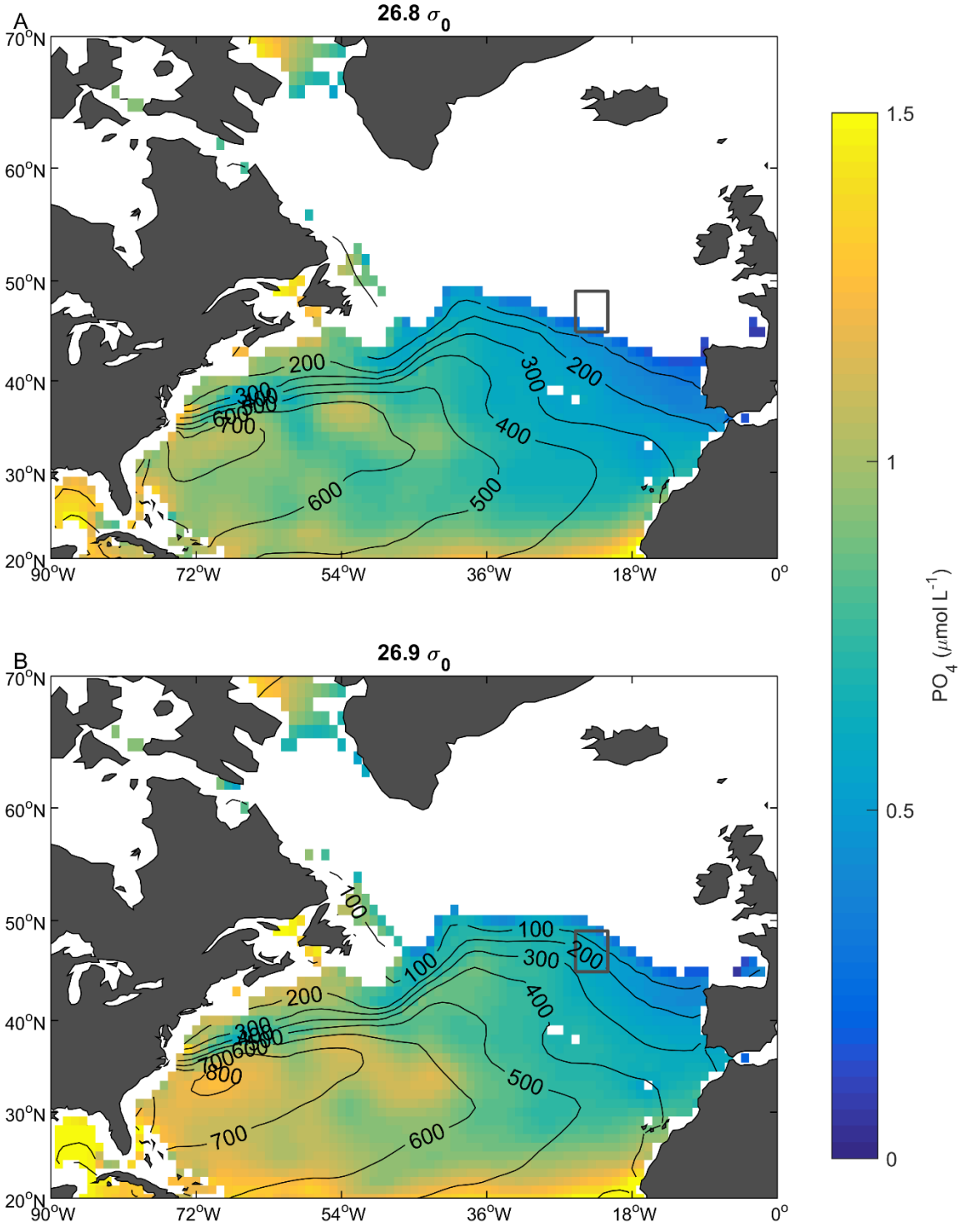
A
26.8 σ_0
70°N
60°N
50°N
40°N
30°N
20°N
90°W
72°W
54°W
36°W
18°W
0°
200
300
400
500
600
700
B
26.9 σ_0
100
200
300
400
500
600
700
800
1.5
1
0.5
0
PO_4 (μmol L^{-1})

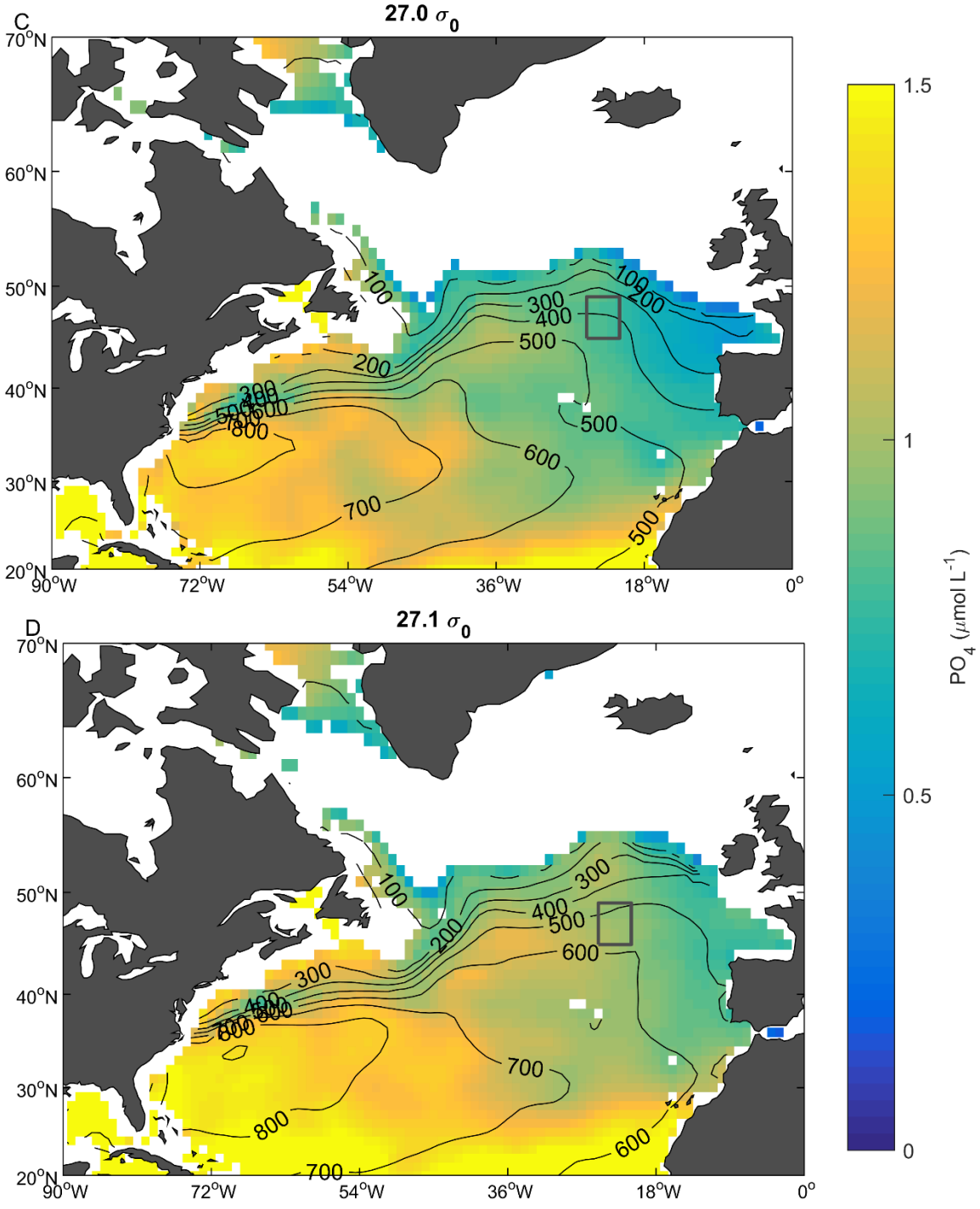
C
27.0 σ_0
70°N
60°N
50°N
40°N
30°N
20°N
90°W
72°W
54°W
36°W
18°W
0°
100
200
300
400
500
600
700
800
D
27.1 σ_0
1.5
1
0.5
0
PO_4 (μmol L^{-1})

Figure 3.2. Winter positions of nutrient tube isopycnals. Annual climatological mean phosphate concentrations (shading) are shown, projected onto the winter (DJF) positions of the A) 26.8, B) 26.9, C) 27.0, and D) 27.1 σ_0 isopycnals. Contours show the vertical depth of each isopycnals. The representative intergyre region is boxed in gray. All data from World Ocean Atlas objectively analyzed mean fields.

concentrations persist northward.

Previous work has shown that some portion of Gulf Stream nutrients are advected into the subpolar gyre [*Williams et al.*, 2011], near-surface waters north of the intergyre region originate in the Gulf Stream [*Burkholder and Lozier*, 2014], and nutrient bearing isopycnals within the Gulf Stream outcrop within the depth of the winter mixed layer in the intergyre (Figure 3.2). However, we have not established a direct pathway between the nutrient-bearing Gulf Stream and the intergyre.

3.2. Methods

To determine pathways for nutrient supply to the base of the winter mixed layer in the intergyre, we use 3-day outputs spanning the time period 1990-2004 from the FLAME general circulation model [*Böning et al.*, 2006]. 75,000 synthetic floats were seeded in the intergyre region, between 100 and 400 m depth, and advected in reverse using a Runge-Kutta 4th-order method. This method is identical to that used in Burkholder and Lozier [2014] to diagnose the deep Gulf Stream origin of the near-surface waters north of the intergyre region. Heatmaps of float displacement were then computed, by gridding the ocean into 0.5x0.5° bins, and counting the total number of floats in each bin after 1, 2, 3, and 4 years of advection. Similar heatmaps were computed

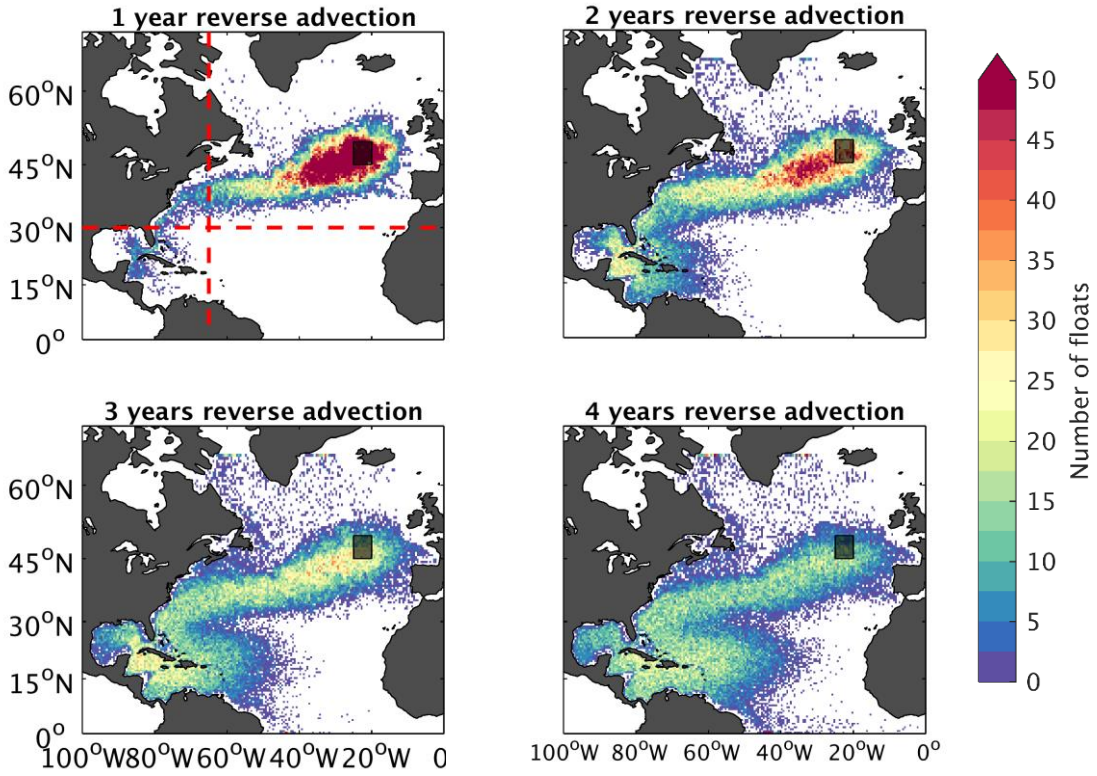

Figure 3.3. Planview heat maps of float positions after 1, 2, 3, and 4 years of reverse advection in the FLAME general circulation model. Shading shows the number of floats in each 0.5°x0.5° grid cell. 75,000 synthetic floats were seeded in the representative intergyre region (boxed), between 100 and 400 m depth (the approximate range between the summer and winter mixed layers.

for the first crossing by each float of the 30° N line of longitude, and the 65° W line of latitude, on a 1°x50 m grid.

3.3. Results

Advected float pathways are strongly associated with the average position of the Gulf Stream and North Atlantic Current (Figure 3.3). After 1 year of advection, most floats are still east of 40° W, though some have reached as far as the Straits of Florida. After 2 years of advection, more floats have reached the coast of North America, and

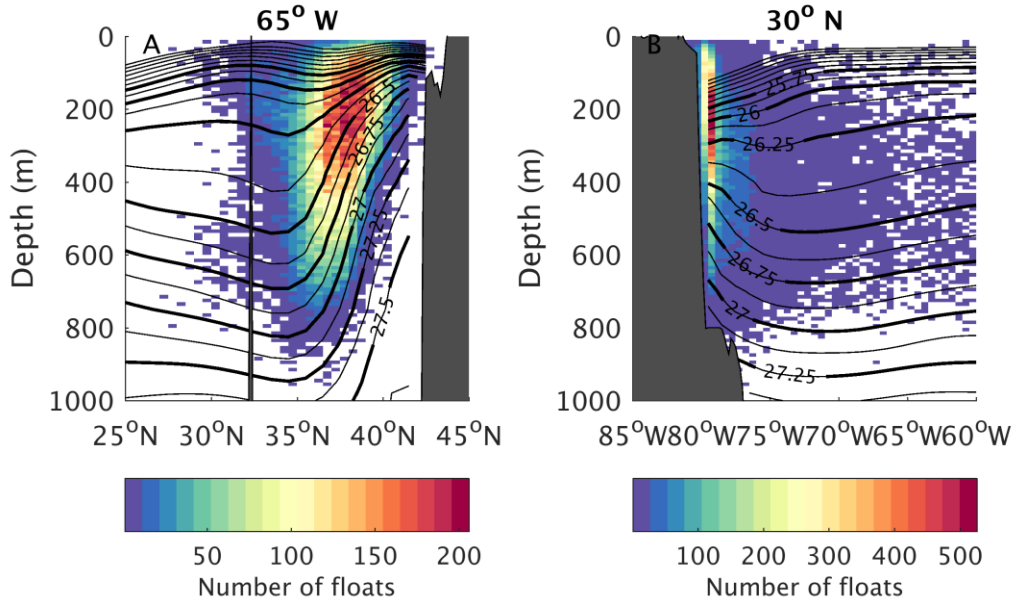

Figure 3.4. Cross-section heat maps of float positions when their trajectories first cross A) 65° W, and B) 30° N. All floats are seeded in the intergyre, at 100-400 m depth in the FLAME general circulation model. Shading shows the number of floats in each 0.5°x10 m grid cell. Contours show the annual climatological mean positions of the 25.75 to 27.5 σ_0 isopycnals. Hydrographic data from World Ocean Atlas. The topographic anomaly in A) at 32° N is Bermuda.

some appear to have spread into the subtropical gyre. After 3 and 4 years of reverse advection, similar patterns continue. Floats continue to be advected primarily along the North Atlantic Current and Gulf Stream, with a small number spreading into the subpolar gyre. After reaching the Gulf Stream, it appears that most floats then spread into the subtropical gyre.

Most floats cross 65° W between 100 and 400 m depth, between the 26.0 σ_0 and 27.0 σ_0 isopycnals, and north of 35° N (Figure 3.4a). A small number of floats cross south of 35° N, but virtually all floats cross 65° W north of 35° N. Furthermore, the

climatological sloping position of Gulf Stream isopycnals can be seen to be highly associated with increased float crossings. Crossings of the 30° N line of latitude occur primarily onshore, between 100 and 400 m depth (Figure 3.4b).

3.4. Discussion

The reverse float study clearly shows that waters within the depth of the winter mixed layer in the intergyre originate in the Gulf Stream, and are transported via the AMOC. In the horizontal, float trajectories are strongly associated with the average path of the Gulf Stream and North Atlantic Current. Crossings of the 65° W line of longitude and the 35° N line of latitude show float positions moving preferentially toward the coast as they move upstream. Most floats seeded in the intergyre cross these boundary lines at shallower depths and on lighter isopycnals than are associated with the nutrient tube, specifically the portion of the nutrient tube thought to pass through to the subpolar gyre [*Pelegrí and Csanady,* 2011; *Williams et al.*, 2011]. The observational record shows isopycnals shoaling consistent with the delivery of Gulf Stream isopycnals to the intergyre.

The inferred along-isopycnal connection from the observational record, as well as the model-derived transport throughput between the deeper Gulf Stream and the intergyre provide evidence that Gulf Stream nutrients are delivered to the base of the intergyre mixed layer. Winter mixing supplies these nutrients to the surface, where they

are made available to phytoplankton in the euphotic zone to fuel the summer growing season.

4. Conclusions

The intergyre region relies on the seasonal entrainment of nutrients to fuel the spring phytoplankton bloom. The convergence of the advective and diffusive fluxes are not large enough to explain the observed levels of export production. There are likely errors in the flux calculations presented here, resultant from both the methodology chosen to calculate the mixed layer depth, as well as the estimates used from NCP. However, these errors do not change the largely one-dimensional view of nutrient supply in the intergyre. On seasonal timescales, primary production in the North Atlantic intergyre is maintained by the seasonal entrainment of nutrients at depth to within the mixed layer.

The nutrients at the base of the mixed layer likely originate within the nutrient-bearing Gulf Stream, on the other side of the North Atlantic, transported to the intergyre by the AMOC. The climatological positions of the 26.8-27.1 σ_0 isopycnals, as well as previous modeling studies, suggest a pathway for Gulf Stream nutrients to shoal to within the mixed layer as they move northward. Float studies provide strong evidence that near-surface waters within the intergyre originate almost entirely within the Gulf Stream. On seasonal timescales, it is clear that mixing drives nutrient supply in the intergyre. However, on longer timescales it is possible that upstream processes in the AMOC might hold implications for intergyre nutrient concentrations. Changes in

nutrient delivery to the tropical AMOC, or changes in the path of the AMOC itself, might all cause changes in nutrient concentrations in the intergyre.

Previous work has suggested that a future ocean, warmed by climate change and more increasingly stratified, might be one in which nutrients will become less accessible and ocean productivity will slow [*Doney*, 2006]. However, more recent work focusing on lower latitude, subtropical oceans has shown that on interannual timescales, there is not a strong relationship between stratification and chlorophyll *a* [*Dave and Lozier*, 2012; *Lozier et al*., 2011]. Such results would seem to cast doubt on the role of mixing in establishing variability in phytoplankton growth in nutrient-limited systems, but the intergyre is distinct both physically and biologically from the subtropical gyre [*Henson et al*., 2009]. These differences allow for the possibility that, while mixing might not drive interannual variability in the subtropical gyre, a stronger relationship might exist between stratification and primary production in the intergyre.

References

Abernathy, R. P., and J. Marshall (2013), Global surface eddy diffusivities derived from satellite altimetry, *J. Geophys. Res. Oceans*, *118*, 901-916, doi:10.1002/jgrc.20066.

Aumont, O., C. Ethé, A. Tagliabue, L. Bopp, and M. Gehlen (2015), PISCES-v2: an ocean biogeochemical model for carbon and ecosystem studies, *Geosci. Model Dev.*, *8*, 2465-2513.

Barton, A. D., M. S. Lozier, and R. G. Williams (2015), Physical controls of variability in North Atlantic phytoplankton communities, *Limonol. Oceanogr.*, *60*, 181-197.

Behrenfeld, M. J. (2010), Abandoning Sverdrup's critical depth hypothesis, *Ecology*, *91*, 977-989.

Behrenfeld, M. J., and P. G. Falkowski (1997), Photosynthetic rates derived from satellite-based chlorophyll concentration, *Limnol. Oceanogr.*, *42*(1), 1-20.

Brambilla, A. and L. D. Talley (2006), Surface drifter exchange between the North Atlantic subtropical and subpolar gyres. *J. Geophys. Res.*, *111*, C07026, doi:10.1029/2005JC003146.

Brody, S. R., and M. S. Lozier (2014), Changes in dominant mixing length scales as a driver of subpolar phytoplankton bloom initiation, *Geophys. Res. Lett.*, *41*, 3197-3203.

Broecker, W. S. (1991), The Great Ocean Conveyor, *Oceanography*, *4*, 79-89.

Burkholder, K. C., and M. S. Lozier (2011), Subtropical to subpolar pathways in the North Atlantic: Deductions from Lagrangian trajectories, *J. Geophys. Res.*, *116*, C07017, doi:10.1029/2010JC006697.

Burkholder, K. C., and M. S. Lozier (2014), Tracing the pathways of the upper limb of the North Atlantic Meridional Overturning Circulation, *Geophys. Res. Lett.*, *41*, 4254-4260, doiL10.1002/2014GL060226.

Chiswell, S. M., P. H.R. Calil, and P. W. Boyd (2015), Spring blooms and annual cycles of phytoplankton: a unified perspective, *J. Plankton Res.*, *32*(3), 500-508.

Cole, S. T., C. Wortham, E. Kunze, and W. B. Owens (2015), Eddy stirring and horizontal diffusivity from Argo float observations: Geographic and depth variability, *Geophys. Res. Lett.*, *42*, 3989-3997, doi:10.1002/2015GL063827.

Dave, A. C., and M. S. Lozier (2015), The impact of advection on stratification and chlorophyll variability in the equatorial Pacific, *Geophys. Res. Lett.*, *42*, 4523-4531, doi:10.1002/2015GL063290.

Dave, A. C., A. D. Barton, M. S. Lozier, and G. A. McKinley (2015), What drives seasonal change in oligotrophic area in the subtropical North Atlantic? *J. Geophys. Res. Oceans*, *120*, 3958-3969, doi:10.1002/2015JC010787.

de Boyer Montégut, C., G. Madec, A. S. Fischer, A. Lazar, and D. Iudicone (2004), Mixed layer depth over the global ocean: An examination of profile data and a profile-based climatology. *J. Geophys. Res.*, *109*, C12, doi:10.1029/2004JC002378.

Doney, S. C. (2006), Oceanography-Plankton in a warmer world, *Nature*, *444*(7120), 695-696, doi:10.1038/444695a.

Eppley, R. W., and B. J. Peterson (1979), Particulate organic matter flux and planktonic new production in the deep ocean, *Nature*, *282*, 677-680.

Foukal, N. P., and M. S. Lozier (2016), On the propagation of sea-surface temperature anomalies from the subtropical gyre to the subpolar gyre in the North Atlantic, *Nature Communications*, doi:10.1002/2016GL068303.

Fratantoni, D. M. (2001), North Atlantic surface circulation during the 1990s observed with satellite-tracked drifters, *J. Geophys. Res.*, *106*, 22067-22093.

Gregg, M. C. (1987), Diapycnal mixing in the thermocline: A review, *J. Geophys Res. Oceans*., 92, 5249-5286.

Gruber, N., C. D. Keeling, and N. R. Bates (2002), Interannual variability in the North Atlantic Ocean carbon sink, *Science*, *298*, 2374-2378.

Henson, A. A., J. P. Dunne, and J. L. Sarmiento (2009), Decadal variability in North Atlantic phytoplankton blooms, *J. Geophys. Res.*, *114*, C04013, doi:10.1029/2008JC005139.

Holte, J. and L. Talley (2006), A new algorithm for finding mixed layer depths with applications to Argo data and Subantarctic mode water formation, *J. Atmos. Oceanic Technol.*, *26*, 1920-1939.

Kara, A. B., P. A. Rochford, and H. E. Hurlburt (2000), An optimal definition for ocean mixed layer depth, *J. Geophys. Res.*, *105*, C7, 16,803-16,821.

Laws, E. A. (1991), Photosynthetic quotients, new production and net community production in the open ocean, *Deep Sea Res., Part A*, *38*(1), 143-167.

Laws, E. A., P. G. Falkowski, W. O. Smoth, H. Ducklow, and J. J. McCarthy (2000), Temperature effects on export production in the open ocean, *Global Biogeochem. Cycles*, *14*, 1231-1246.

Laws, E. A., E. D'Sa, and P. Naik (2011), Simple equations to estimate ratios of new or export production to total production from satellite-derived estimates of seas surface temperature and primary production, *Limnol. Oceanogr. Methods*, *9*(12), 593-601.

Ledwell, J. R., A. J. Watson, and C. S. Law (1997), Evidence for slow mixing across the pycnocline from an open-ocean tracer-release experiment, *Nature*, *364*, 701-703.

Letscher, R. T., F. Primeau, and J. K. Moore (2016), Nutrient Budgets in the subtropical ocean gyres dominated by lateral transport, *Nature Geoscience*, *9*, 815-819, doi:10/1038/NGE02812.

Li, Z., and N. Cassar (2016), Satellite estimates of net community production based on O_2/Ar observations and comparison to other estimates, *Global Biogeochem. Cycles*, *30*, 735-742.

Lozier, M. S., A. C. Dave, J. B. Palter, L. M. Gerber, and R. T. Barber (2011), On the relationship between stratification and primary productivity in the North Atlantic, *Geophys. Res. Lett.*, *38*, L18609, doi:10.1029/2011GL049414.

Palter, J. B., and M. S. Lozier (2008), On the source of Gulf Stream nutrients, *J. Geophys. Res.*, *113*, C06018, doi:10.1029/2007JC004611.

Palter, J. B., M. S. Lozier, and R. T. Barber (2005), The effect of advection on the nutrient reservoir in the North Atlantic subtropical gyre, *Nature*, *437*, 687-692.

Pelegrí, J. L. and G. T. Csanady (1991), Nutrient transport and mixing in the Gulf Stream, *J. Geophys. Res.*, *96*, C2, 2577-2583.

Qu, T. (2003), Mixed layer heat balance in the western North Pacific, *J. Geophys. Res.*, *108*, C7, doi:10.1029/2002JC001536.

Redfield, A. (1934), On the proportions of organic derivatives in sea water and their relation to the composition of plankton. In Daniel R. J. (ed James Johnstone Memorial Volume), University Press of Liverpool, 177-192.

Sverdrup, H. (1953), On conditions for the vernal blooming of phytoplankton, *J. Conseil. Int. Explot. Mer.*, *18*, 287-295.

Taylor, J. R., and R. Ferrari (2011), Shutdown of turbulent convection as a new criterion for the onset of spring phytoplankton blooms, *Limnol. Oceanogr.*, *56*(6), 2293-2307.

Williams, R. G., E. McDonagh, V. M. Roussenov, S. Torres-Valdes, B. King, R. Sanders, and D. A. Hansell (2011), Nutrient streams in the North Atlantic: Advective pathways of inorganic and dissolved organic nutrients, *Global Biogeochem. Cycles*, *25*, GB4008, doi:10.1029/2010GB003853.

Williams, R. G., V. Roussenov, and M. J. Follows (2006), Nutrient streams and their induction into the mixed layer, *Global Biogeochem. Cycles*, *20*, doi:10.1029/2005GB002586.

Wu, J., W. Sunda, E. A. Boyle, and D. M. Karl (2000), Phosphate depletion in the western North Atlantic Ocean, *Science*, *289*, 759-762, doi:10.1126/science:289.5480.759.